

Note: Molecular dynamics studies of high-density amorphous ice: Influence of long-range Coulomb interactions

Markus Seidl,^{1,2} Ferenc Karsai,² Thomas Loerting,¹ and Gerhard Zifferer^{2,a)}

¹Institute of Physical Chemistry, University of Innsbruck, Innrain 52a, A-6020 Innsbruck, Austria

²Department of Physical Chemistry, University of Vienna, Währinger Str. 42, A-1090 Wien, Austria

(Received 31 October 2011; accepted 20 December 2011; published online 13 January 2012)

[doi:10.1063/1.3676058]

Apart from at least 16 (crystalline) ice phases supercooled water exists in several amorphous states which may be structurally characterized, e.g., by X-ray powder diffraction and distinguished by their density ρ at 1 bar.¹ Low-density amorphous ice (LDA) has a density of $\rho = 0.94$ g/cm³, high-density amorphous ice (HDA) of $\rho = 1.13$ – 1.15 g/cm³, and very high-density amorphous ice (VHDA) of $\rho = 1.26$ g/cm³. These three states can be transformed into each other by amorphous-amorphous transitions.^{2,3} A theoretical key question is, if amorphous ices are glasses rather than nanocrystalline materials. A route toward an answer is to study their behavior during heating/cooling cycles which is quite different for glasses and crystalline materials: only glasses show a so-called glass transition. In the region of the glass transition temperature T_g glasses become softer and transform to a supercooled (and ultraviscous) liquid upon heating. Therefore, if HDA for example shows a glass transition it represents the glassy state of a corresponding liquid state called high-density liquid (HDL).⁴ Both the glassy and the liquid state are metastable with respect to crystalline phases. By contrast to experiments, in molecular dynamics simulations crystallization is avoided due to the ultrahigh heating/cooling rates employed. Thus, they provide highly efficient routes for the investigation of properties of amorphous species.⁵ For example, for HDA at a pressure of $p \approx 0.3$ GPa a glass transition was observed⁶ with T_g depending on the model as well as (slightly) on the evaluation method adopted: from the density profile (enthalpy, onset of pronounced increasing mobility) $T_g \approx 184$ K (178 K, 182 K) for COMPASS, ≈ 194 K (190 K, 192 K) for TIP3P*, and ≈ 223 K (214 K, 219 K) for SPC/E*. Force field COMPASS (Ref. 7) is a commercial class-II force field optimized for the simulation of condensed phases and TIP3P* and SPC/E* are representatives with flexible bonds and bond angles of the common force fields TIP3P⁸ and SPC/E⁹ having fixed geometries.

In the present note we extend our earlier calculations⁶ to a different treatment of Coulomb interactions motivated by Ref. 10, which gives emphasis to the importance of introducing long-range Coulomb interactions.

Comparison of the critical point of the liquid-liquid transition of ST2 water regarding long-range Coulomb interactions by Ewald summation to a study with truncated electrostatic interactions¹¹ reveals only one critical point at $T = 237$ K instead of three at 235 K, 260 K, and 275 K.¹⁰ Thus, although the possibility of introducing some artificial

ordering in amorphous systems by Ewald summation cannot be definitely excluded,¹² it is a highly interesting task to investigate its influence on properties of HDA models. In addition, we study the influence of different heating/cooling rates on the basic simulation data and on T_g .

The method adopted is described in Ref. 6 and only briefly reproduced here for convenience of the reader: Constant pressure and temperature molecular dynamics simulations (NpT) are performed by use of Materials Studio[®] 4.4 from Accelrys Inc. applying the Verlet velocity algorithm with a time step of 1 fs under control of the Andersen thermostat and barostat applying the module Discover. In the first set of calculations a cut-off distance of 1.25 nm with a spline switching function (0.3 nm width) is applied for the non-bonding interactions making use of charge groups (as in our previous communication, but with different heating/cooling rates; see below). In the second set for the Coulomb part long-range terms are regarded by use of Ewald summation.

A box with 1024 water molecules (periodic boundary conditions) is prepared at the experimental density of HDA at 1 bar and the initial system is produced by several nanoseconds NpT relaxation at the target temperature 80 K and pressure 0.3 GPa. Then, the system is repeatedly heated in steps of 10 K until a maximum temperature (300 K) is reached and then cooled to 80 K. At each temperature a 50 ps (“fast”) run is performed—corresponding to a heating/cooling rate of 2×10^{11} K/s—using the first half of the trajectory for equilibration and the second for data sampling.

The calculated quantities comprise density $\rho(T)$ in g cm⁻³, enthalpy $H(T)$ in kJ mol⁻¹ (calculated from the simulations as the sum of potential energy, kinetic energy, and pV) and the mean square displacement $msd_{15}(T)$ of oxygen atoms within 15 ps, shown in Fig. 1 for force field COMPASS omitting the first (relaxation) cycle.

First, the simulation results (set 1, truncated interactions) are compared to our former simulations with 500 ps (“slow”) runs,⁶ corresponding to a ten times slower heating/cooling rate. For all profiles the data from “slow” (marked green in Fig. 1) and “fast” (blue symbols) runs are closely related and T_g calculated from individual profiles, e.g., $\rho(T)$ vs. T for 500 ps and 50 ps runs, respectively, are similar. Not unexpectedly slightly larger T_g values are obtained for the 50 ps runs, caused by a tiny shift of densities toward smaller values at low temperatures, see Fig. 1 and Table I. The effect of a ten times faster heating/cooling rate on raw data and T_g , however,

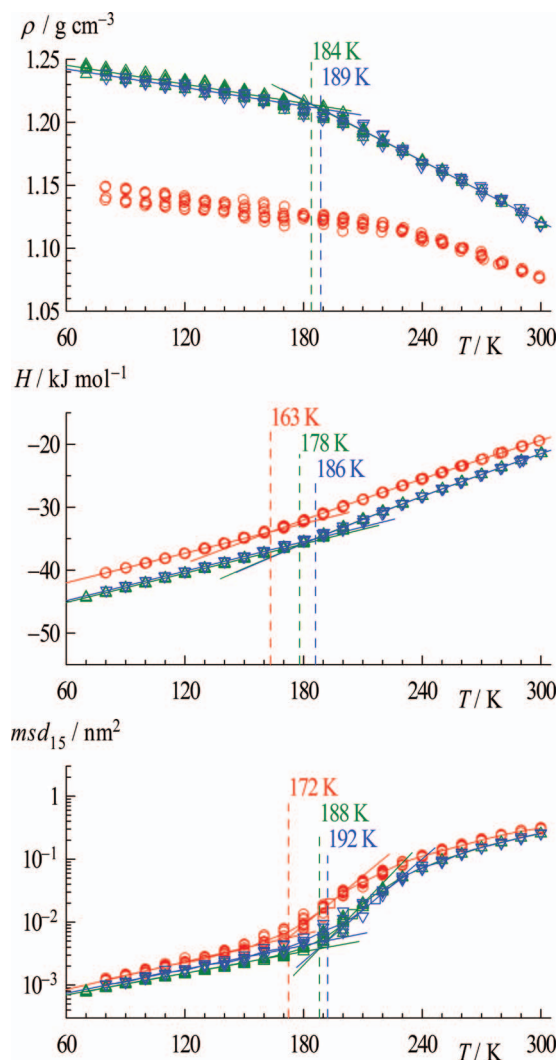


FIG. 1. Density ρ (top), enthalpy H (middle), and mobility msd_{15} (bottom) vs. temperature T , force field COMPASS, 50 ps/10 K, truncated Coulomb interactions (blue) and Ewald summation (red). Data for 500 ps/10 K, truncated Coulomb interactions (green) are taken from Ref. 6. Squares in the bottom diagram indicate points of inflection.

is rather small. Thus, the much more time consuming calculations with Ewald summation (set 2, depicted in red in Fig. 1) are restricted to runs with 50 ps per individual temperature.

Applying Ewald summation the density at 80 K is $\approx 0.10 \text{ g cm}^{-3}$ lower compared to truncated Coulomb interactions. Upon heating the decrease of ρ is less pronounced, the difference in densities at 300 K being $\approx 0.04 \text{ g cm}^{-3}$. As lower densities are correlated with larger average distances between molecules, the enthalpy and mobility are slightly increased. T_g may be easily extracted from the enthalpy traces, which show a downshift of ca. 20 K compared to truncated Coulomb interactions, being compatible with results obtained from the onset of increased mobility. No pronounced kink appears in the $\rho(T)$ vs. T curves. Instead increased fluctuations followed

TABLE I. Densities at 80 K and 300 K, first neighbor coordination number N for oxygen atoms at 80 K (within the range 0.25–0.34 nm) and (averaged) glass transition temperatures T_g obtained for 50 ps/10K.

	Group based cut-off				Ewald summation			
	$\rho/\text{g cm}^{-3}$		N	T_g/K	$\rho/\text{g cm}^{-3}$		N	T_g/K
	80 K	300 K			80 K	300 K		
COMPASS	1.24	1.12	5.5	189	1.14	1.08	4.7	167
SPC/E*	1.23	1.15	5.5	235	1.14	1.11	4.7	200
TIP3P*	1.28	1.16	6.2	207	1.20	1.11	5.3	178

by a plateau are found near T_g evaluated from the enthalpy H . Analysis of the pair distribution functions (not shown) reveals also a slight effect, especially to the first neighbor coordination number of oxygen atoms which is slightly smaller if Ewald summation is applied (see Table I).

In summary, T_g depends on the force field, the treatment of Coulomb interactions and to some extent on the heating/cooling rate. All models clearly suggest the existence of a glass transition from high-density amorphous ices (HDA, VHDA) to ultraviscous high-density liquids (HDL, VHDL) at low temperatures (160–240 K), thus corroborating the interpretation of recent experimental dilatometry curves of HDA (Ref. 13) at 2 K/min which yield a glass transition temperature of $142 \pm 2 \text{ K}$ at 0.3 GPa by defining the onset of deviation from linearity as $T_{g,\text{onset}}$.

We are grateful to the Austrian Academy of Sciences (ÖAW-DOC grant to M.S.) and the European Research Council (ERC Starting Grant SULIWA to T.L.) for financial support.

^{a)} Author to whom correspondence should be addressed. Electronic mail: gerhard.zifferer@univie.ac.at.

¹T. Loerting, K. Winkel, M. Seidl, M. Bauer, C. Mitterdorfer, P. H. Handle, C. G. Salzmann, E. Mayer, J. L. Finney, and D. T. Bowron, *Phys. Chem. Chem. Phys.* **13**, 8783 (2011).

²O. Mishima, *J. Chem. Phys.* **100**, 5910 (1994).

³T. Loerting, V. V. Brazhkin, and T. Morishita, *Adv. Chem. Phys.* **143**, 29 (2009).

⁴P. G. Debenedetti, *J. Phys.: Condens. Matter* **15**, R1669 (2003).

⁵N. Giovambattista, C. A. Angell, F. Sciortino, and H. E. Stanley, *Phys. Rev. Lett.* **93**, 047801 (2004).

⁶M. Seidl, T. Loerting, and G. Zifferer, *J. Chem. Phys.* **131**, 114502 (2009).

⁷D. Rigby, *Fluid Phase Equilib.* **217**, 77 (2004).

⁸W. L. Jorgensen, J. Chandrasekhar, J. D. Madura, R. W. Impey, and M. L. Klein, *J. Chem. Phys.* **79**, 926 (1983).

⁹H. J. C. Berendsen, J. R. Grigera, and T. P. Straatsma, *J. Phys. Chem.* **91**, 6269 (1987).

¹⁰Y. Liu, A. Z. Panagiotopoulos, and P. G. Debenedetti, *J. Chem. Phys.* **131**, 104508 (2009).

¹¹I. Brovchenko, A. Geiger, and A. Oleinikova, *J. Chem. Phys.* **123**, 044515 (2005).

¹²S. Boreesch and O. Steinhäuser, *Ber. Bunsenges. Phys. Chem.* **101**, 1019 (1997).

¹³M. Seidl, M. S. Elsaesser, K. Winkel, G. Zifferer, E. Mayer, and T. Loerting, *Phys. Rev. B* **83**, 100201 (2011).